



THE STUDY OF LONGITUDINAL AND LATITUDINAL VARIATION OF EQUATORIAL ELECTROJET SIGNATURE AT STATIONS WITHIN THE 96°MM AND 210°MM AFRICAN AND ASIAN SECTORS RESPECTIVELY UNDER QUIET CONDITIONS.

*Akpaneno, A. F., Joshua Matthew and Ekundayo, K. R.

Department of Physics, Federal University Dutsin-Ma, Katisna State

*Corresponding author's Email: aakpaneno@fudutsinma.edu.ng

ABSTRACT

Solar quiet current (S_q) and Equatorial Electrojet (EEJ) are two current systems which are produced by electric current in the ionosphere. The enhancement of the horizontal magnetic field is the EEJ. This research is needed for monitoring equatorial geomagnetic current which causes atmospheric instabilities and affects high frequency and satellite communication. This study presents the longitudinal and latitudinal variation of equatorial electrojet signature at stations within the 96°mm and 210°mm African and Asian sectors respectively during quiet condition. Data from eleven observatories were used for this study. The objectives was to determine the longitudinal and latitudinal geomagnetic field variations during solar quiet conditions, Investigate monthly variation and diurnal transient seasonal variation; Measure the strength of the EEJ at stations within the same longitudinal sectors and find out the factors responsible for the longitudinal and latitudinal variation of EEJ. Horizontal (H) component of geomagnetic field for the year 2008 from Magnetic Data Acquisition System (MAGDAS) network were used for the study. The International Quiet Days (IQDs) were used to identify quiet days. Daily baseline values for each of the geomagnetic element H were obtained. The monthly average of the diurnal variation was found. The seasonal variation of dH was found. Results showed that: The longitudinal and latitudinal variation in the dH differs in magnitude from one station to another within the same longitude due to the difference in the influence of the EEJ on them.

Keywords: Equatorial Electrojet, Counter Electrojet, Ionosphere

INTRODUCTION

One of the interesting geophysical phenomena associated with the equatorial ionosphere is the enhancement of geomagnetic variations on the ground at the equatorial stations when compared to those at off-equatorial latitudes. This phenomenon named by Chapman (1951) as “equatorial electrojet” (EEJ) is observed on a variety of periodicities in the geomagnetic field. The general explanation of this effect is that the two dimensional current system in the sun lit part of the E -region of the ionosphere has a narrow band of enhanced current density almost parallel to the dip equator approximately in the west-east direction. If one assumes that the vertical currents are zero then the anisotropic Cowling conductivity in the equatorial region becomes large thereby producing a strong but narrow current band known as equatorial electrojet. Therefore any geomagnetic variation which is due to the currents in the E -region is expected to show EEJ enhancement. The equatorial electrojet (EEJ) is a strong ionospheric current along the magnetic equator driven by the day side eastward electric field. The worldwide solar-driven wind results in the S_q (solar quiet) current system in the E region of the Earth's ionosphere (100–130 km altitude). Resulting from this current is an electrostatic field directed E-W (dawn-dusk) in the equatorial day side of the ionosphere. At the magnetic dip equator, where the geomagnetic field is horizontal, this electric field results in an enhanced eastward current flow within ± 3 degrees of the magnetic equator, known as the equatorial electrojet (Roy, 1998).

The equatorial electrojet is usually eastward during the daytime. However, there are occasionally days when geomagnetic data indicate a westward current flow, typically lasting for a few hours. The reversed flow of the equatorial electrojet is called counter electrojet (Yamazaki *et al.*, 2012a). Modeling studies have shown that a particular combination of tidal mode scan result in a counter electrojet (Forbes and Lindzen, 1976b; Takeda and Maeda, 1981; Hanuise *et al.*, 1983). The study performed by Raghavarao and Anandarao (1980) showed that an upward wind with a sufficiently large magnitude (15–20 m/s) can also cause a counter electrojet. Observational studies have found that the occurrence of CEJ is dependent on the phase of the moon, suggesting that lunar tides play a role (Bartels and Johnston, 1940; Rastogi, 1974; Sastri and Arora, 1981). Other studies found that a large-magnitude CEJ event during winter is often observed during a stratospheric sudden warming event, suggesting a physical connection between the two phenomena (Stening *et al.*, 1996; Sridharan *et al.*, 2009; Fejer *et al.*, 2010). A quiet-time CEJ event is often accompanied by unusual S_q variations at other latitudes, indicating that a CEJ is a result of a large-scale process (Stening, 1977b; Bhargava and Sastri, 1977). Global ionospheric current systems during the occurrence of CEJ events were examined by several authors (e.g., Takeda and Maeda, 1980b; Rastogi, 1994; Gurubaran, 2002; Yamazaki *et al.*, 2012a). Those studies revealed the presence of additional current systems that are superposed on the normal S_q current system. During geomagnetically active periods, a counter electrojet is sometimes caused by the penetration of the polar-region electric field to equatorial latitudes (Rastogi and Patel,

1975; Rastogi, 1997; Kikuchi *et al.*, 2003, 2008). Besides, storm time thermospheric winds tend to drive a westward electric field in the dayside equatorial region through the mechanism known as *disturbance dynamo* (Blanc and Richmond, 1980; Fuller-Rowell *et al.*, 2002). The effect of the disturbance dynamo reduces or sometimes even reverses the eastward electric field produced by normal quiet-time winds. The disturbance dynamo electric field can persist for several days after geomagnetic activity quiets down, and thus can result in a reduced *EEJ* or *CEJ* during the recovery phase of a storm (Le Huy and Amory-Mazaudier, 2005; Yamazaki and Kosch, 2015). Recently, Vineeth *et al.*, (2016) reported a remarkable correlation between the monthly mean meteor counts and the number of afternoon *CEJ* events during 2006–2007. Their observations are consistent with the numerical results by Muralikrishna and Kulkarni (2008), which predicted that a dust-particle layer of meteoric origin could cause a reversal of the vertical polarization electric field in the equatorial electrojet

Previous studies on the longitudinal variability of the equatorial electrojet (*EEJ*) and the occurrence of its counter electrojet (*CEJ*) using the available records of the horizontal component *H* of the geomagnetic field simultaneously recorded in the year 2009 (mean annual sunspot number $R_z = 3.1$) along the magnetic equator in the South American, African, and Philippine sectors. The results indicate that the *EEJ* undergoes variability from one longitudinal representative station to another, with the highest value of about 192.5 nT recorded at the South American sector at Huancayo and a minimum peak of 40.7 nT at Ilorin in western Africa. Obtained longitudinal inequality in the *EEJ* was explicable in terms of the effects of local winds, dynamics of migratory tides, propagating diurnal tide, and meridional winds. The African stations of Ilorin and Addis Ababa registered the greatest percentage of *CEJ* occurrence. Huancayo in South America, with the strongest electrojet strength, was found to have the least occurrence of the *CEJ*. It is suggested that activities that support strong *EEJ* inhibits the occurrence of the *CEJ*. Percentage of occurrence of the *CEJ* varied with seasons across the longitudes. The order of seasonal variation of morning occurrence does not tally with the evening occurrence order at any station. A semiannual equinoctial maximum in percentage of morning occurrence of the *CEJ* was obtained at Huancayo and Addis Ababa. Only Addis Ababa recorded equal equinoctial maxima in percentage of evening occurrence of the *CEJ*. The seasonal distribution of the occurrences of the *CEJ* at different time regimes implies a seasonal variability of causative mechanisms responsible for the occurrence of the *CEJ* (Rabiu, *et al.*, 2017).

In years back, since the discovery of *EEJ* which is located along the dip equator, many researches have been carried out in order

to understand fully the characteristics and properties this band of eastward current. Also results from research carried out by Khashba, *et al.*, (2015) reveals that there is a local time dependence of *EEJ*. The *EEJ*-related magnetic effects in the daily variations of the horizontal component appear at about 0600 LT, reach maximum near local noon and vanish after 1800 LT. Simultaneous surface magnetic records from eight stations in different longitude sectors were used to study the longitudinal dependence of *EEJ* for three separately analyzed years. The intensity of *EEJ* was found to be stronger in South America with a maximum at about $77^\circ W$. It is followed by a minimum in West Africa at about $4^\circ E$. The *EEJ* magnetic signature is relatively weak in Asia with a minimum in India between 70° and $90^\circ E$. A secondary maximum is about $125^\circ E$. These longitude variations of the *EEJ* magnetic effect roughly follow variation of the inverse main field ($1/B$) at the dip equator.

Under quiet geomagnetic conditions the variations of the three geomagnetic elements *H*, *Z*, and *D* from one day to the next in June, October, and December 1986 at eight Indian observatories from about 0° to 22° dip latitude was studied. The day to day variability was also measured by sequential variability, *SV*(1). In all the three months, the magnitude of day to day variability in *H*, *Z*, and *D* had a diurnal variation with maximum around local noon and minimum in the night. This is most likely controlled by the diurnal variation of ionospheric conductivity. In the worldwide part of S_q (WS_q) zone, the *SV* in *H*, *Z*, and *D* was smaller in October than in June and December 1986, but *SV*(*z*) is greater than *SV*(*H*) and *SV*(*D*) in all the three months. In the equatorial electrojet (*EEJ*) zone, the *SV* due to the *EEJ* alone in *H*, *Z*, and *D* is greater in June than in October and December contrary to the seasonal variation of S_q (*H*) and S_q (*Z*) in the *EEJ* zone. The *SV*(*D*) due to the *EEJ* alone had a surprisingly large magnitude. There is evidence that the day to day variability of *EEJ* and the WS_q are not in phase and consequently combine somewhat destructively within the *EEJ* Zone. (Okeke *et al.*, 1995).

MATERIALS AND METHODS

Data from 11 MAGDAS (Magnetic Data Acquisition System) stations within 96° and 210° magnetic meridian were obtained in which Ilorin Observatory is one of them (geographic latitude: $8.47^\circ N$, geographic longitude: $4.68^\circ E$, geomagnetic latitude: $1.82^\circ S$, geomagnetic longitude: $78.6^\circ S$) Figure 1. Stations considered were indicated by a cross-sign marking. The MAGDAS data can be used for the study of long-term variations e.g. auroral substorms, magnetic storm, solar quiet S_q , etc. Table 1 shows the coordinates of the stations used in the study.

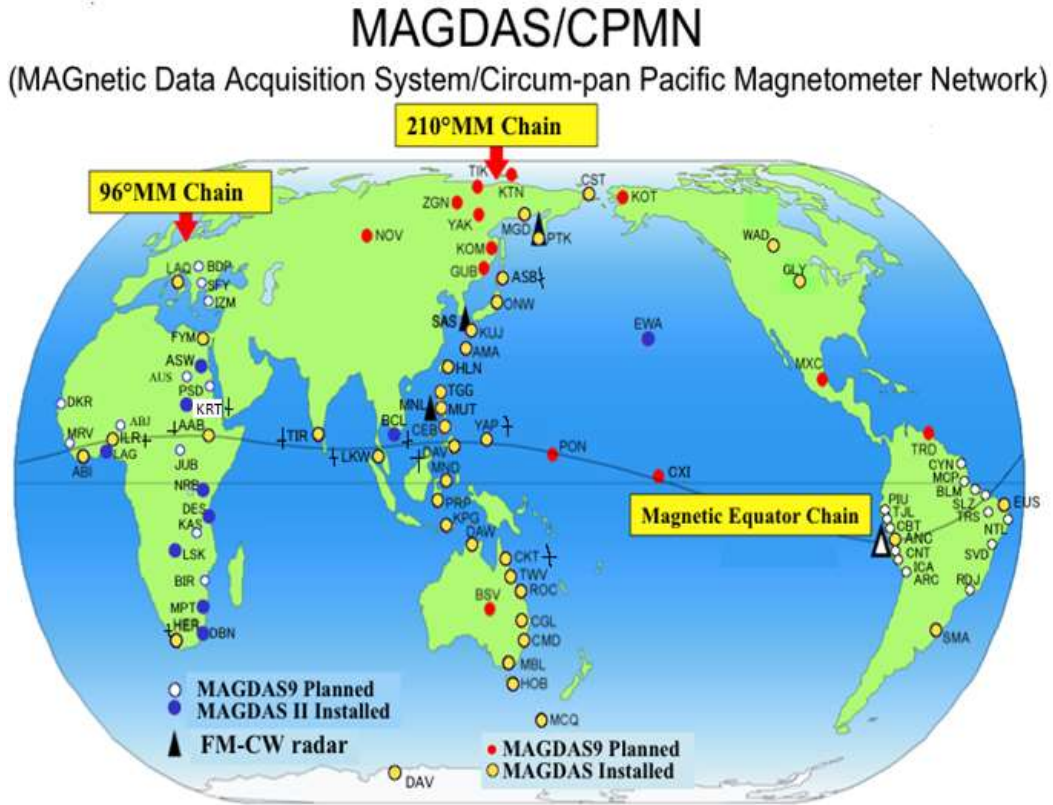


Figure 1 Distribution of the geomagnetic observatories used for the study (Source: Yumoto and MAGDAS Group, 2001)

Table 1: Coordinates for the MAGDAS Stations Used in the Study

S/N	STATIONS	Code	Geographic latitude(°)	Geographic longitude(°)	Geomagnetic latitude(°)	Geomagnetic longitude(°)
1	Ilorin	ILR	8.50	4.68	-1.82	76.8
2	Hermanus	HER	-34.34	19.24	-42.29	82.20
3	Khartoum	KRT	15.33	32.32	5.69	103.8
4	Addis Ababa	AAB	9.04	38.77	0.18	110.23
5	Triunelveli	TIR	8.50	77.0	-1.20	146.40
6	Lang kawi	LKW	6.30	99.77	-1.23	170.06
7	Cebu	CEB	10.36	123.91	2.53	195.06
8	Davao	DAV	7.00	125.40	-1.02	195.54
9	Yap Island	YAP	9.50	138	1.49	209.06
10	Ashibetu	ASB	43.46	142.17	36.43	213.39
11	Cook town	CKT	-15.48	145.25	36.43	213.39

Magnetic data for five quietest days of each month for the year 2008 were selected and used in this study (available at www.ga.gov.au). These days were considered based on magnetic activity index K_p . The K_p index for quietest days are within the range of 0-4. The concept of local time was used throughout the analysis as the stations might be few hours ahead of the Greenwich Meridian Time (G.M.T) or even lagged. The local time relative to GMT for each station is shown in Table 2.

Table 2: The various stations and their corresponding G.M.Ts

STATIONS	AAB	CEB	DAV	ILR	LKW	TIR	YAP	HER	KRT	CKT	ASB
G.M.T	+3	+8	+8	+1	+8	+5	+10	+2	+3	+10	+5

The variation baseline was obtained from 2 hours flanking local midnight i.e. 24 hours' local time (LT) and 1 hour local time. The daily baseline value H_0 for the geomagnetic element H (horizontal component) is the mean value of the hourly values at these two hours

$$H_0 = \frac{1}{2}(H_{24} + H_1) \quad (1)$$

Where H_1 and H_{24} are values of geomagnetic element H at 1hr LT and 24hr LT respectively and H_0 is the daily baseline for the geomagnetic element H which is the mean values of the hourly values at 24hr LT and 1hr LT. The daily baseline H_0 for each station on each quiet day was subtracted from the hourly values H_t to get the hourly departure from the midnight for a particular day. That is;

$$dH = H_t - H_0 \quad (2)$$

Where $t = 1$ to 24

dH gives the measure of the hourly amplitude of the variation of H , which is also the solar daily variation in H ; and $S_q(H)$ is dH during quiet times. The monthly mean values were derived from the mean of the diurnal variations for the five quietest days in each month. The seasonal variation of dH was also investigated. Obtaining the seasonal variation means averaging the monthly mean for Lloyd's season. Lloyd classify the year into three viz:

Equinox Season (March, April, September, and October) denoted as *E-Season*, June solstice (May, June, July and August) as *J-Season* and December solstice (November, December, January and February) as *D-Season*. The seasonal variations for both longitudinal and latitudinal (EEJ strength) variations, was gotten by plotting the average values over monthly mean of the months consisting each season. i.e. the E, J and D seasons.

The EEJ strength was also calculated by subtracting the dH of stations outside the EEJ belt from those within. This is done on both the northern and southern hemispheres after which the diurnal and monthly mean plot was generated using the MATLAB application as well as the contour plot.

RESULTS AND DISCUSSION

The longitudinal geomagnetic field variation during solar quiet condition in dH is shown in Figures 2, 3 and 4 for diurnal basis across all stations with available data. *YAP* shows maximum dH of $94nT$ and minimum dH of $80nT$ at around $1100LT$ and $1200LT$ respectively. *ILR* shows a maximum dH of $65nT$ and minimum dH of $44nT$ at about $1200LT$ and $1100LT$ respectively which is for March Equinox. For September equinox as seen in Figure 1.5 *ILR* has a maximum dH of about $60nT$ and minimum of about $48nT$ at $1000LT$ and $1100LT$ respectively. Also *YAP* has a maximum dH of $90nT$ and minimum dH of $67nT$ at $1100LT$ while $1200LT$ respectively and *AAB* has a maximum dH of about $108nT$ and minimum dH of $78.5nT$ at $1200LT$ and $0100LT$ respectively. Figure 4, *YAP* shows its highest dH value to be $68nT$ and lowest dH value to be $50nT$ both peaking at $1200LT$. *LKW* has a maximum dH to be about $72nT$ and the minimum dH to be $33nT$ at for both. These values shows the variation of dH with longitude diurnally where the highest dH magnitude for the year 2008 was recorded at *DAV* with dH of $108nT$ during the September equinox while the least was

recorded at *LKW* with dH value of $33nT$ during December Solstice.

For latitudinal variation of *EEJ* diurnally as seen in Figures 3, 7 and 11. At April (Equinox month) as seen in Figure 3, the *EEJ* strength at *ILR* compared with *HER* has a maximum value of $57nT$ and minimum value of $50nT$ at $0100LT$ and $1200LT$ respectively. However, the *EEJ* strength at *ILR* compared to *KRT* has a maximum value of $50nT$ and minimum of about $39nT$ both peaking at $1200LT$. The *EEJ* strength at *YAP* compared with *ASB* has its maximum of about $106nT$ and minimum strength of $65nT$ at $1000LT$ and $1100LT$ respectively. The *EEJ* strength at *YAP* as compared with *CKT* shows a maximum dH of $88nT$ and minimum of $75nT$ at $1200LT$ and $1100LT$ respectively.

During the equinox month of October (Figure 7), the *EEJ* strength at *DAV* as compared with *ASB* shows a maximum value of $100nT$ and minimum value of $96nT$ at and both peaking around $1200LT$. *YAP* as compared with *ASB* also shows a maximum *EEJ* strength of $88nT$ and minimum value of $56nT$ both peaking at $1200LT$. *DAV* as compared with *CKT* shows the maximum *EEJ* strength to be about $90nT$ and minimum of $76nT$ both peaking at $1200LT$. *YAP* as compared with *CKT* has a maximum *EEJ* strength of $76nT$ and minimum of $60nT$ at $1100LT$ and $1200LT$ respectively.

During the solstice month of November (Figure 11), *DAV* as compared to *ASB* shows a maximum of dH to $80nT$ and minimum of $58nT$ at $1200LT$ and $1100LT$ respectively, also *DAV* as compared with *CKT* shows *EEJ* strength to have maximum of $73nT$ and minimum of $48nT$ both peaking at $1100LT$, while *EEJ* strength at *AAB* as compared with *HER* is maximum with dH value of $70nT$ and minimum of $42nT$ both peaking at $1200LT$. The result shows that the *EEJ* strength is highest at *YAP-ASB* (i.e the difference in dH between *YAP* and *ASB*) with value of $106nT$ during march equinox. Therefore, it implies that *EEJ* strength is higher in equinoctial months than in solstice months.

The monthly mean (as seen in Figures 4, 8, 12 and 14) show that for the longitudinal variation *ILR* records its highest value of dH in June solstice with value of $75nT$ and least value of $50nT$ in September equinox. *TIR* records its highest dH value to be $92nT$ in September equinox and least value of $50nT$ in December solstice. *AAB* has its highest dH value of $62nT$ at September equinox and least value of $53nT$ in December solstice. *LKW* has its maximum dH value of $77nT$ at September and minimum of $60nT$ in December solstice. *DAV* has its maximum dH value of $92nT$ at September and minimum of $72nT$ in December solstice. *YAP* has its maximum dH value of $87nT$ at March equinox and minimum of $57nT$ in June solstice. *CEB* has its maximum dH value of $87nT$ at March equinox and minimum of $58nT$ in June solstice. This result shows frequent maxima dH occurrence at March equinox while the least occurs at June solstice, it also follows from the daily variation where dH value for longitudinal variation in equinox months is higher than dH in solstice.

The monthly mean for latitudinal variation as seen in the same Figures show that the *EEJ* strength at *ILR* compared with *HER* is maximum in December solstice with dH value of $55nT$ and

minimum in June solstice with dH value of $37nT$. The EEJ strength at ILR compared with KRT is maximum in June solstice with dH value of $43nT$ and minimum in December solstice with dH value of $17nT$. The EEJ strength at YAP compared with ASB is maximum in September equinox with dH value of $76nT$ and minimum in June solstice with dH value of $40nT$. Also the EEJ strength at YAP as compared with CKT is maximum in March equinox with dH value of $80nT$ and minimum in June solstice with dH value of $40nT$. The EEJ strength at DAV compared with ASB is maximum in September equinox with dH value of $93nT$ and minimum in December solstice with dH value of $72nT$. Also the EEJ strength at DAV as compared with CKT is maximum in September equinox with dH value of $78nT$ and minimum in December solstice with dH value of $61nT$. The EEJ strength at AAB as compared with HER is maximum in September equinox with dH value of $60nT$ and minimum in June solstice with dH value of $45nT$. The EEJ strength at AAB as compared with KRT is maximum in June solstice with dH value of $44.5nT$ and minimum in December solstice with dH value of $16nT$.

The seasonal variation as seen from Figures 5, 9, 13 and 14 shows the March equinox, September equinox, December solstice and June solstice respectively. It is notable that from March equinox, March records more EEJ strength ($70nT$) than April ($60nT$) by a difference of $10nT$ which is the range of EEJ

strength for March equinox and the longitudinal variation for the month April has the value of $68nT$ whereas March has a bad data in that respect, hence exempted from the plot. For September equinox; September has more record of EEJ strength ($58nT$) than October ($35nT$) giving the range of EEJ strength in September equinox to have a difference of $23nT$ and for longitudinal variation records October with more dH value ($69nT$) than September ($68nT$) by a slight difference of $1nT$. During June solstice, May has the highest EEJ strength ($40nT$) while August has the least strength ($33nT$) while the highest dH value for longitudinal variation was also recorded at May ($60nT$) and the least was recorded at August ($40nT$). For the December solstice, the month with the highest EEJ strength is February ($87nT$) and the month with least strength is November ($43nT$) while for the longitudinal variation, the highest dH value was recorded in February ($88nT$) and the least was recorded in December ($54nT$).

CEJ event was recorded during pre-sunrise and post-sunset hours where it is more frequent at post sunset. CEJ was seen to occur with its highest amplitude $-76nT$ at about $0800LT$ (Figure 6) The plots all follows the same pattern, rising from pre-sunrise, peaking at around local noon and falls to post sunset hours of the day. In general the S_qH variations were found to be larger before midnight than before sunrise hours.

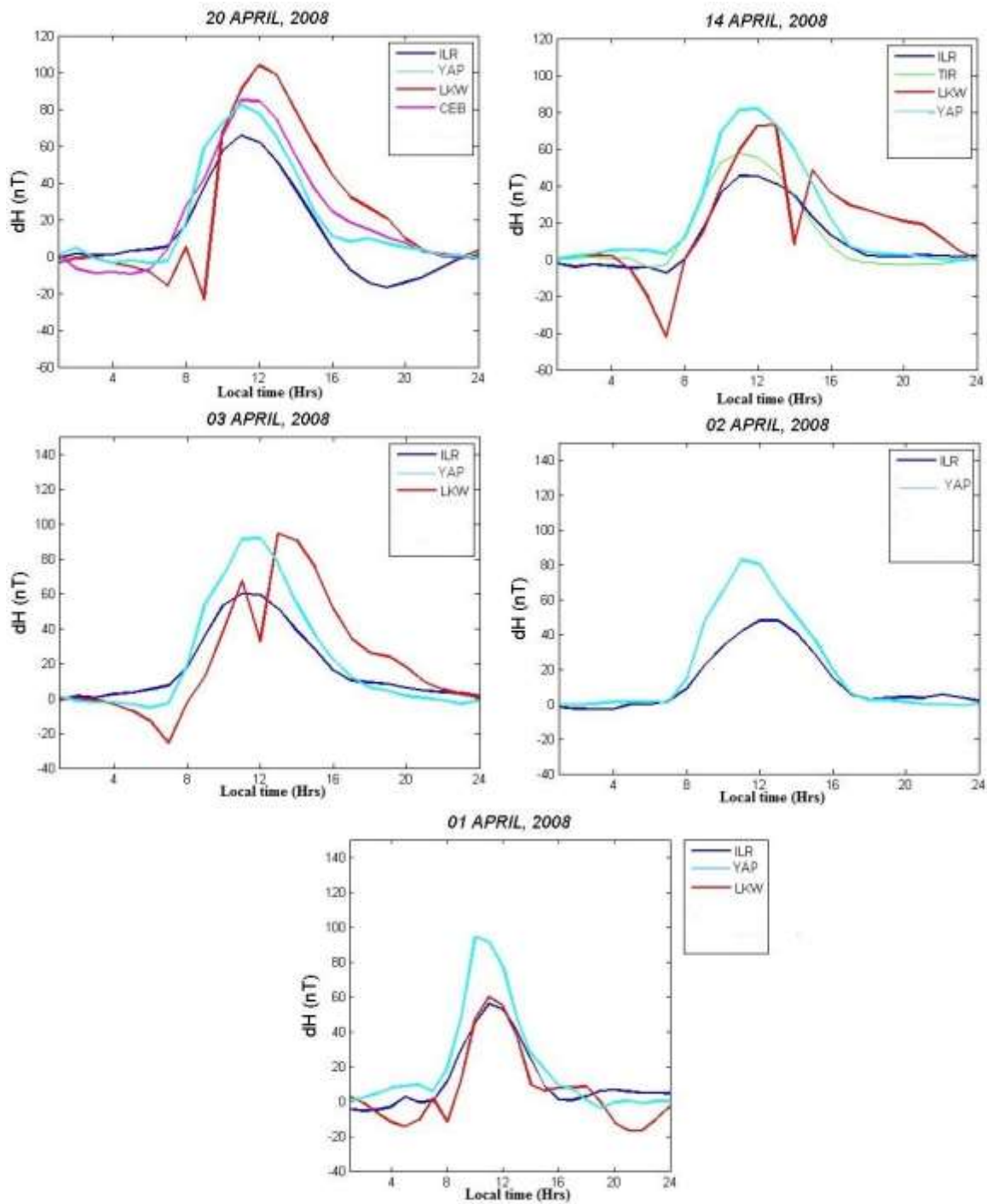


Figure 2: longitudinal variation of EEJ for April

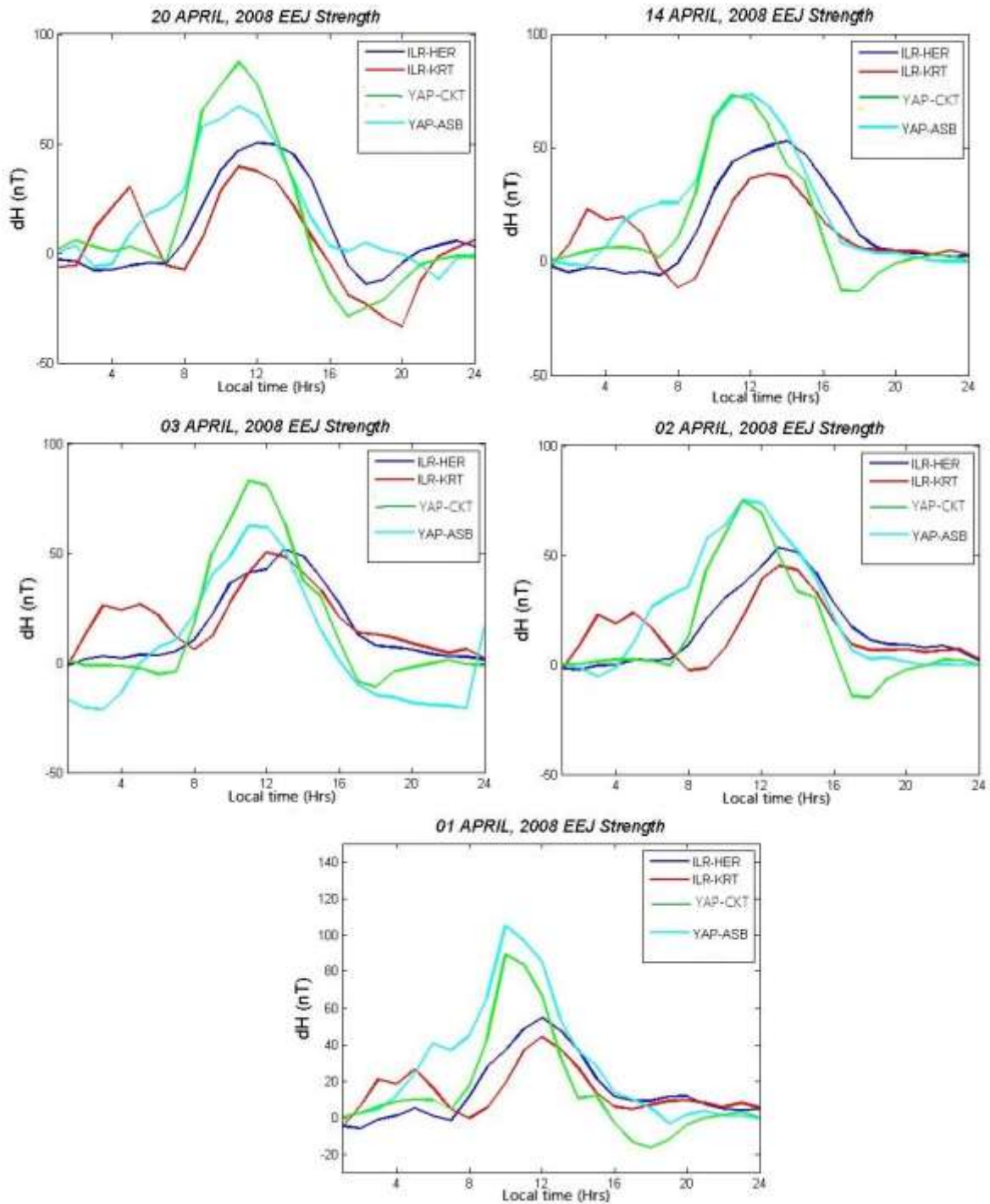


Figure 3: EEJ strength variation for April

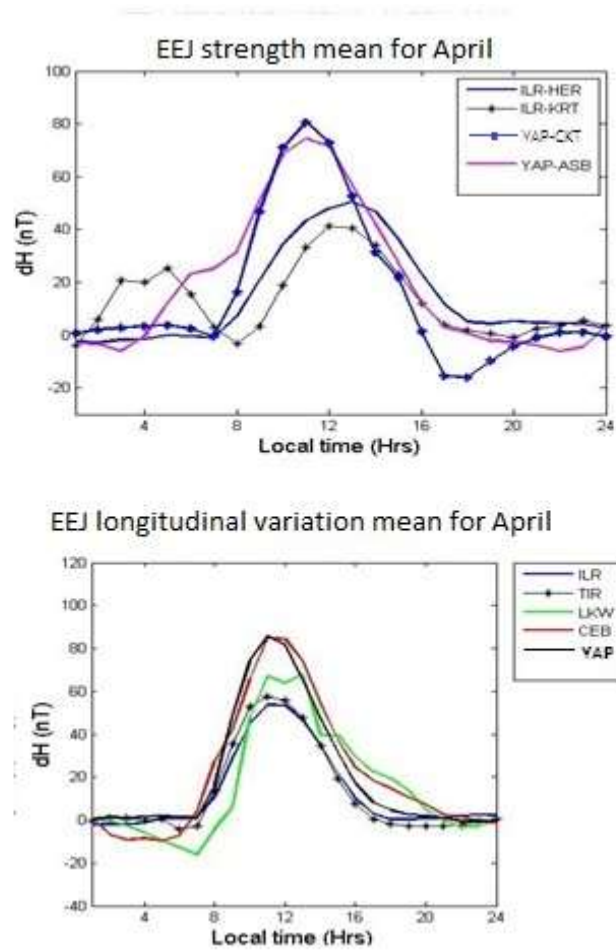


Figure 4: Monthly mean for latitudinal and longitudinal variation of EEJ in April

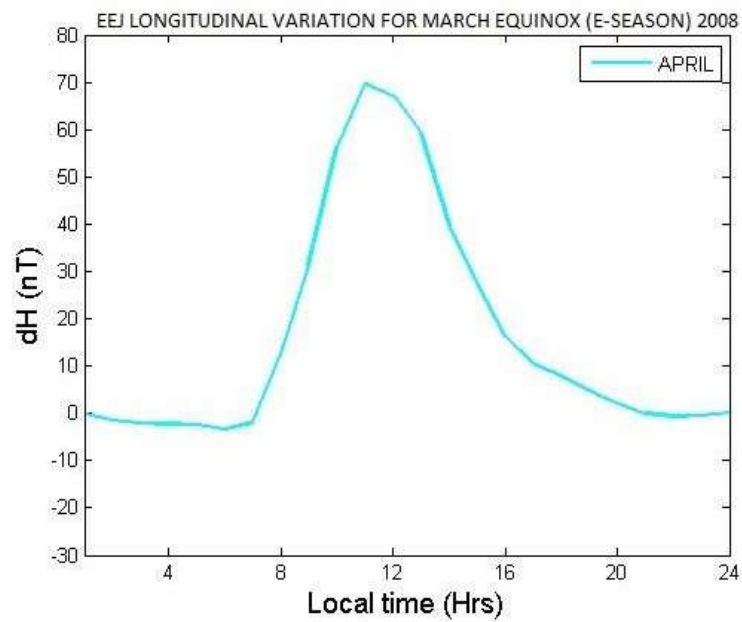
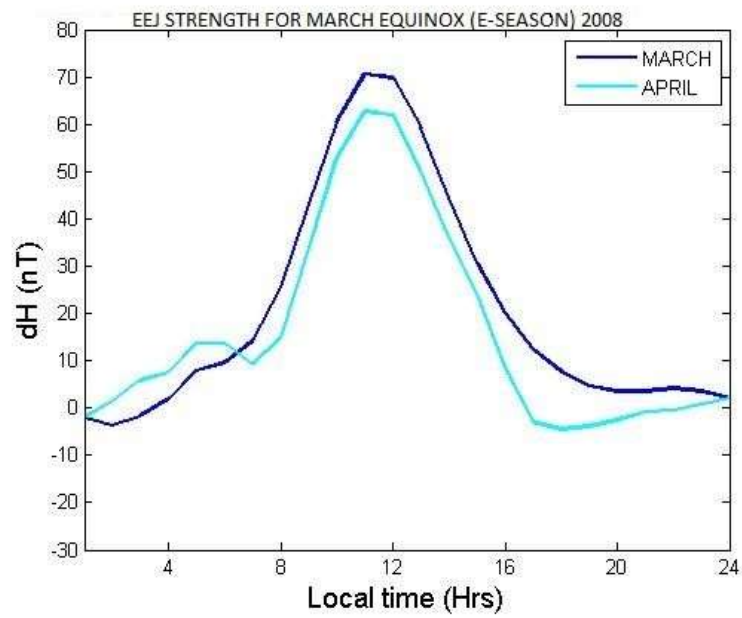


Figure 5 EEJ variation for March Equinox (E-Season)

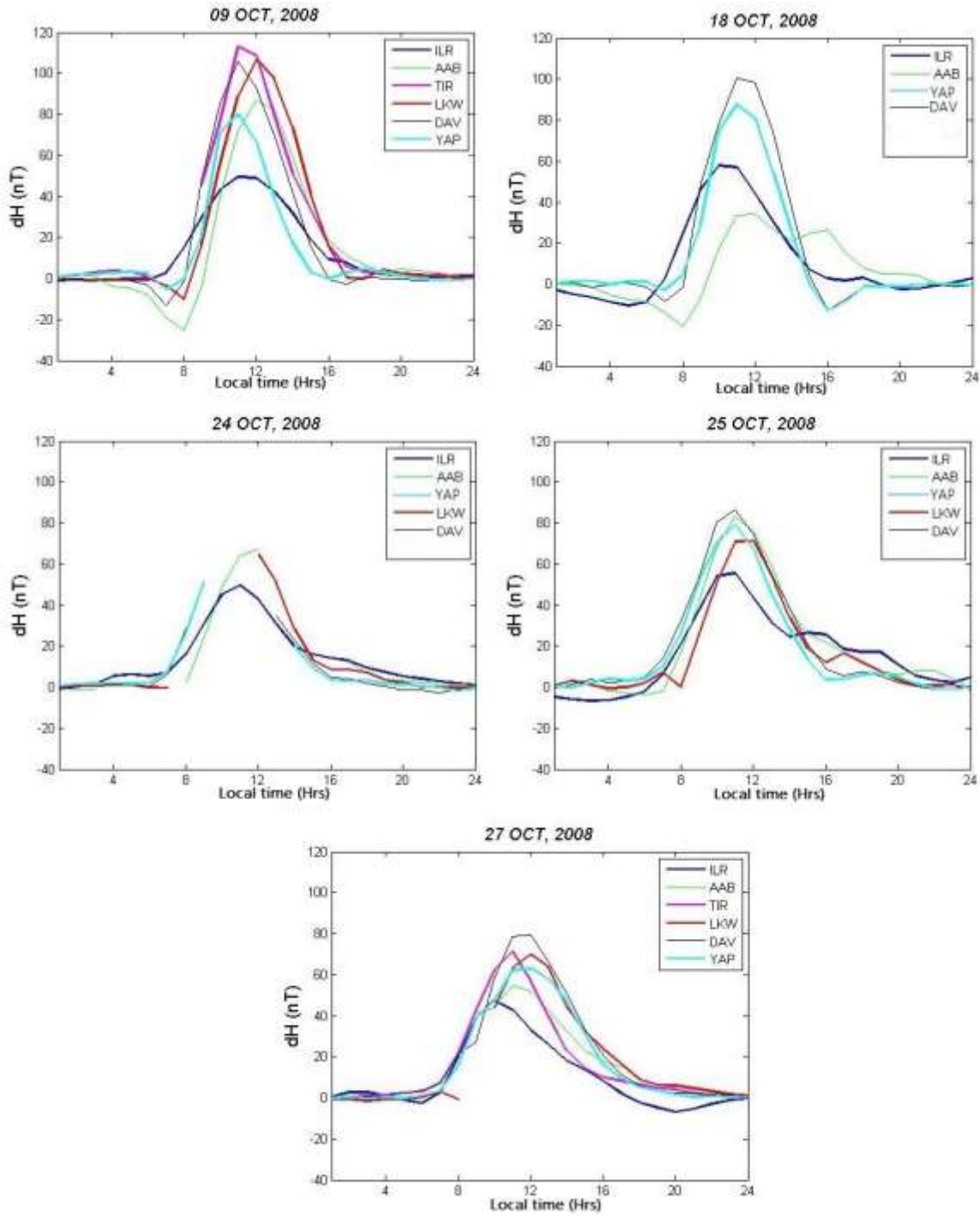


Figure 6: Longitudinal variation of EEJ in October

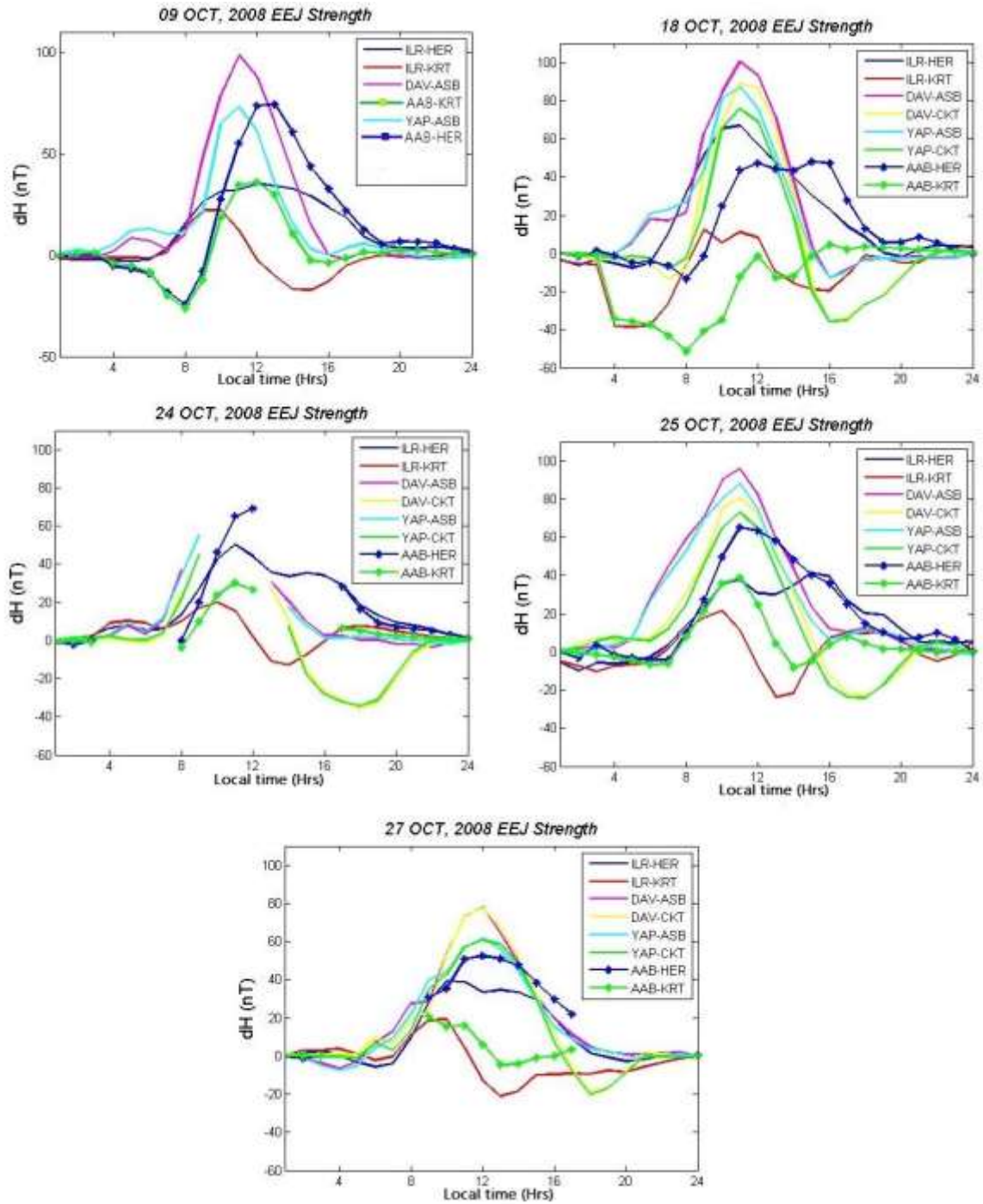


Figure 7: EEJ strength for October

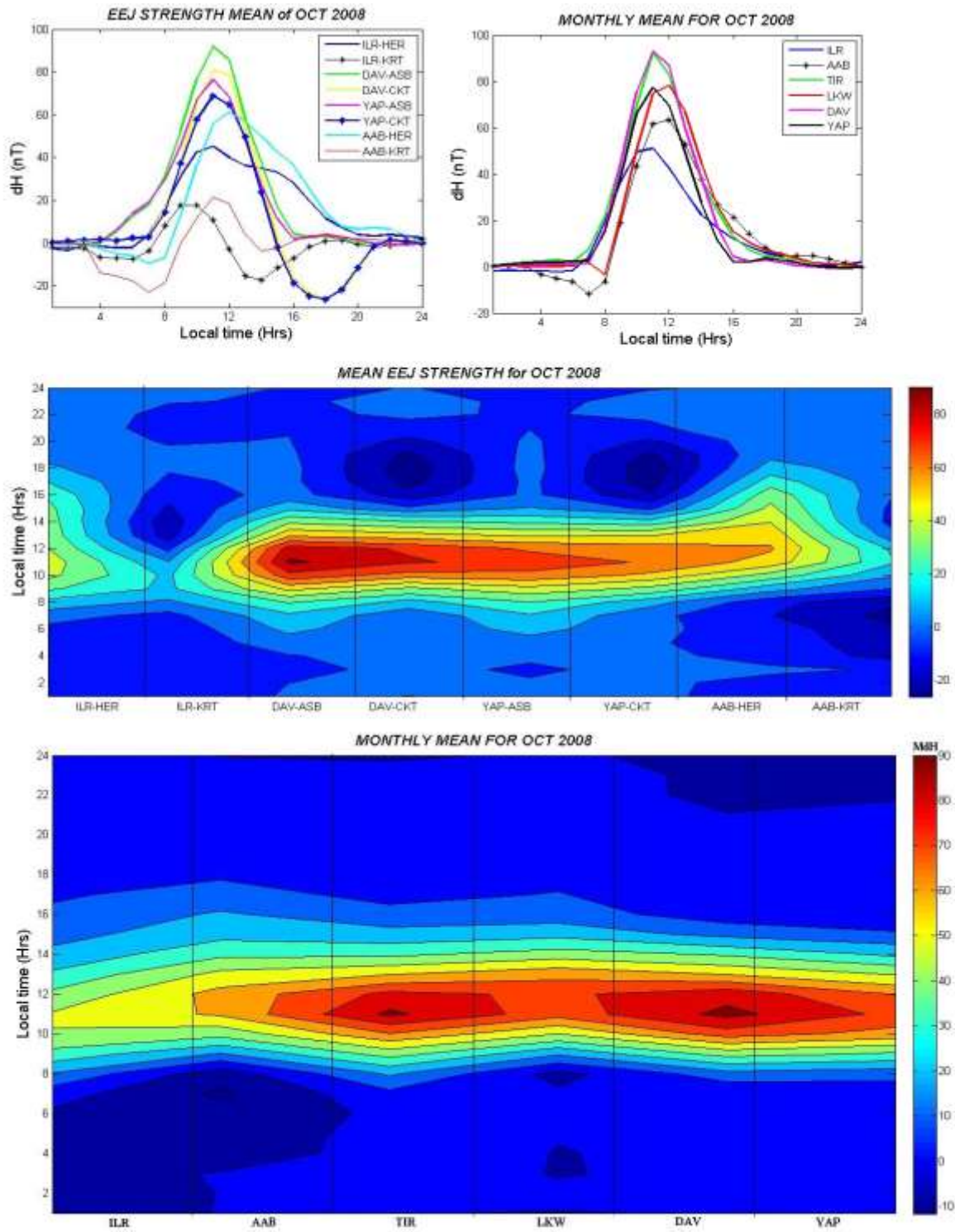


Figure 8: Monthly mean for latitudinal and longitudinal variation of EEJ in October

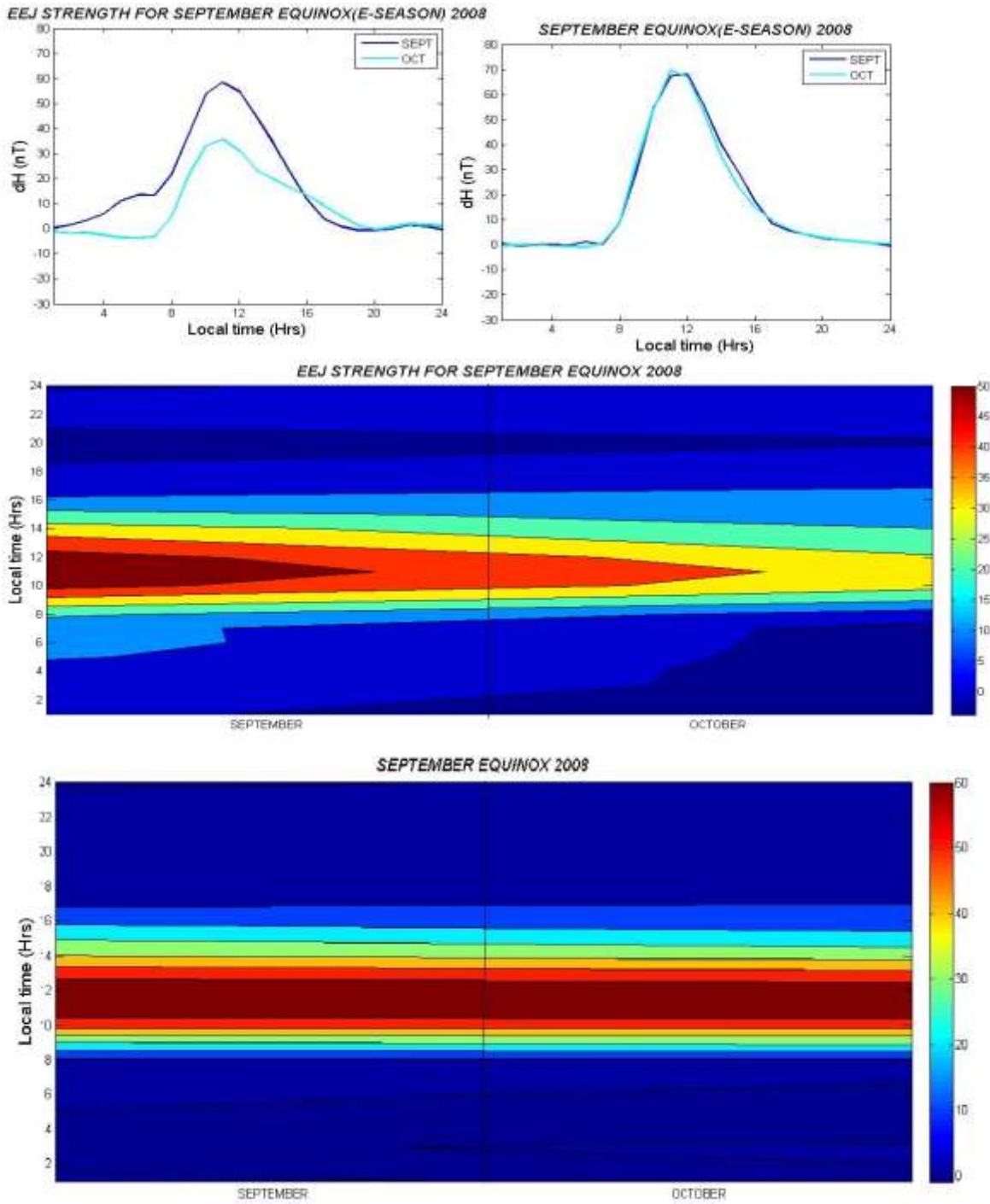


Figure 9: EEJ variation for September equinox (E-Season)

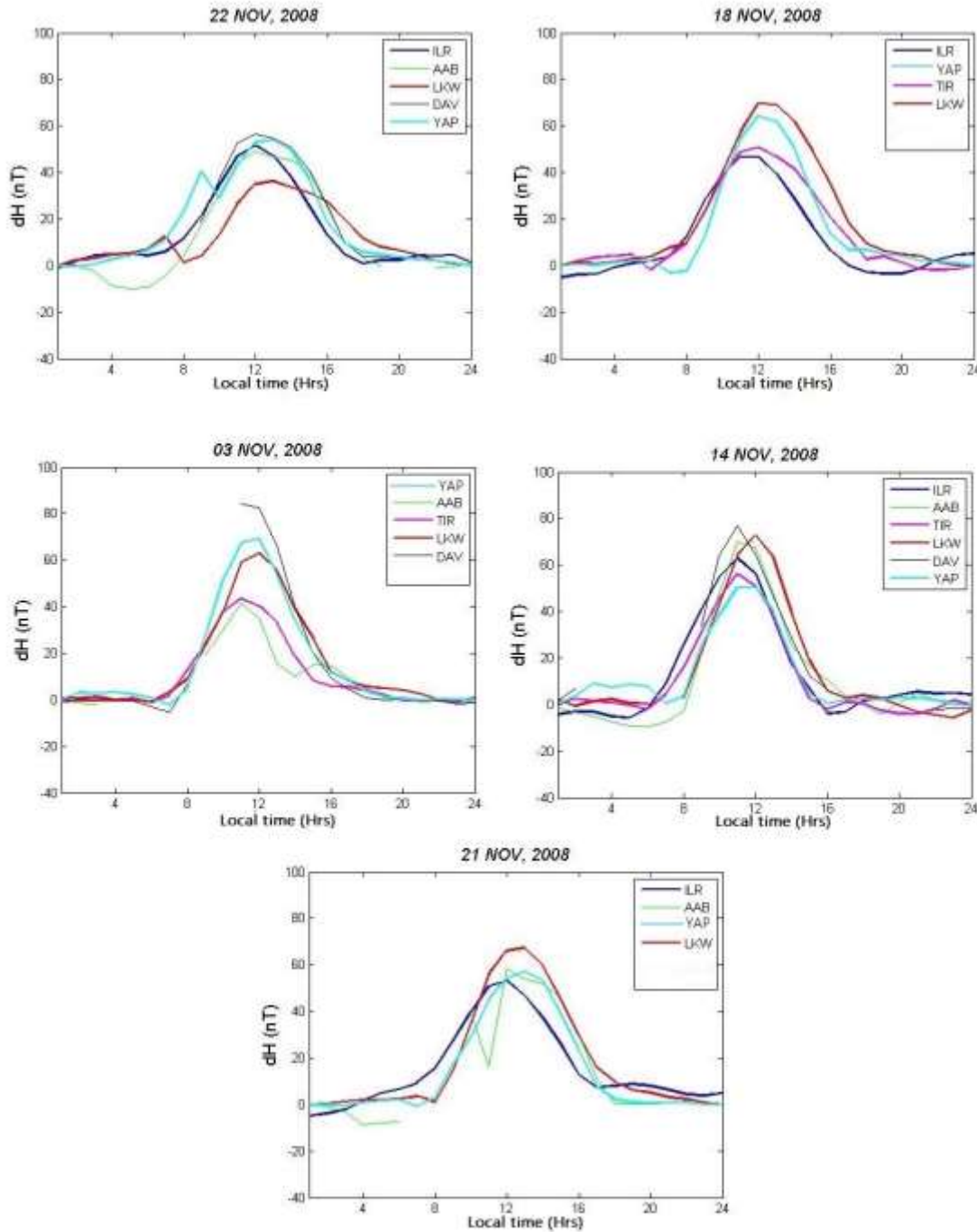


Figure 10: Longitudinal variation of EEJ in November

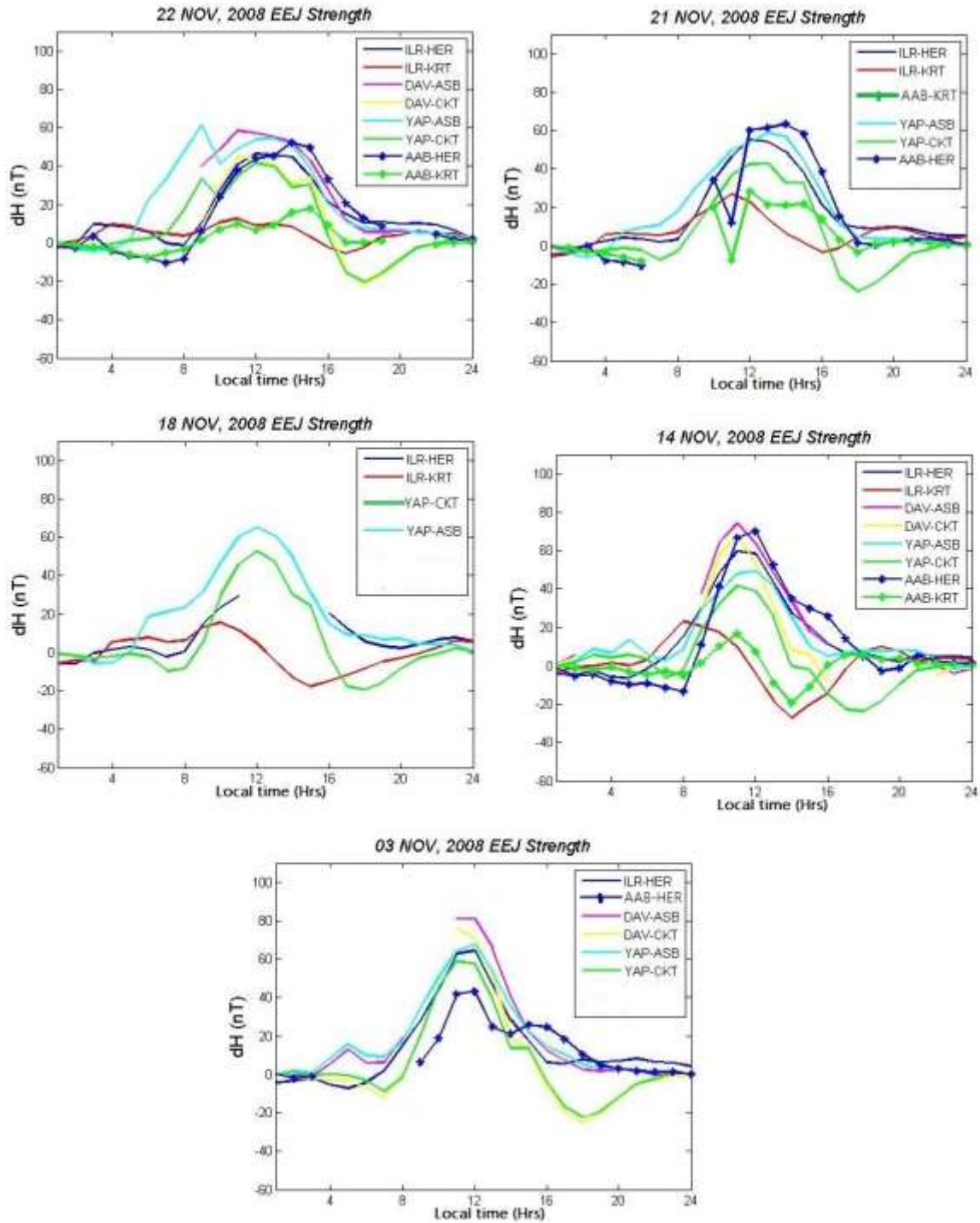


Figure 11: EEJ strength variation for November

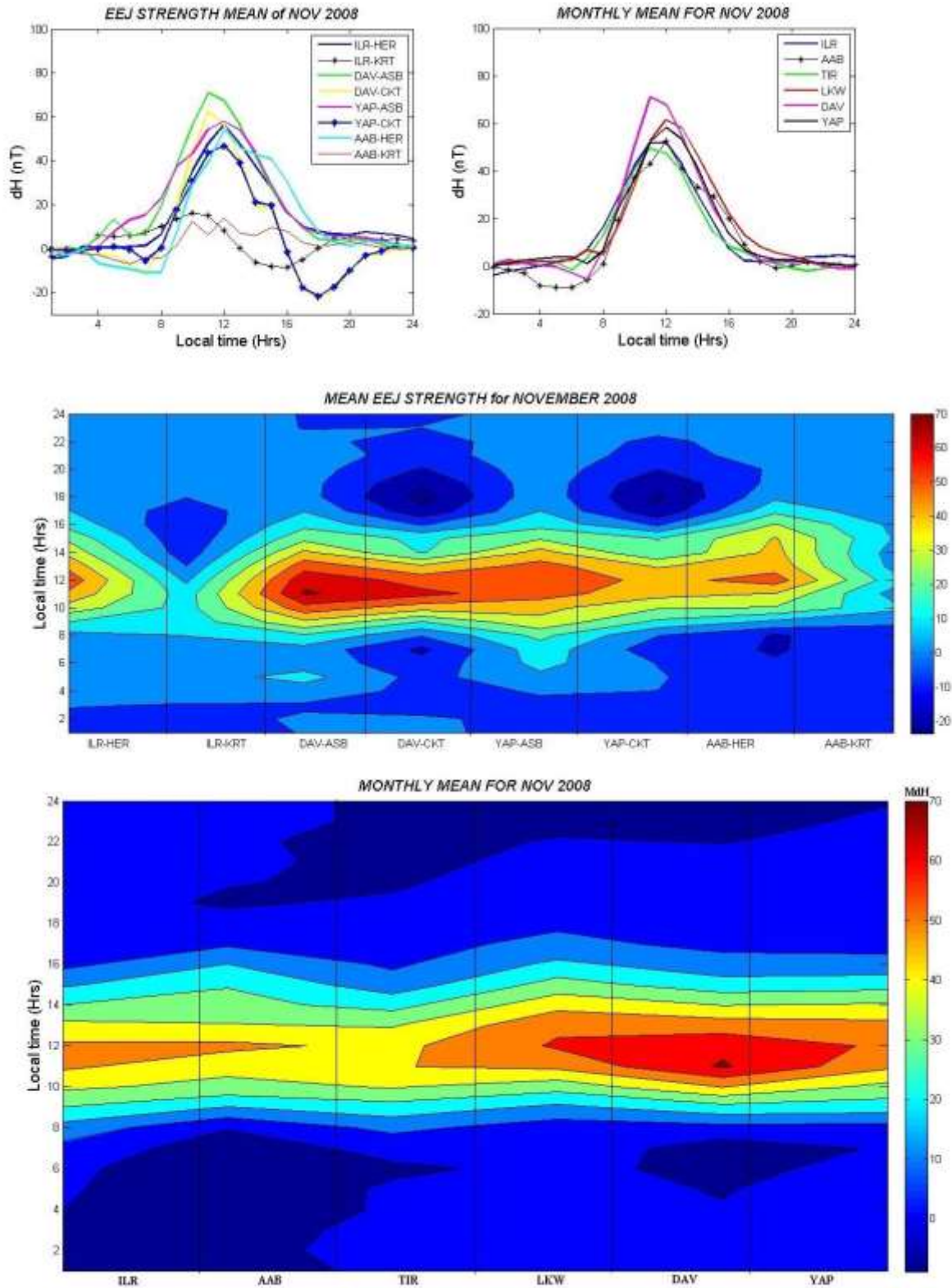


Figure 12: Monthly mean for latitudinal and longitudinal variation of EEJ in November

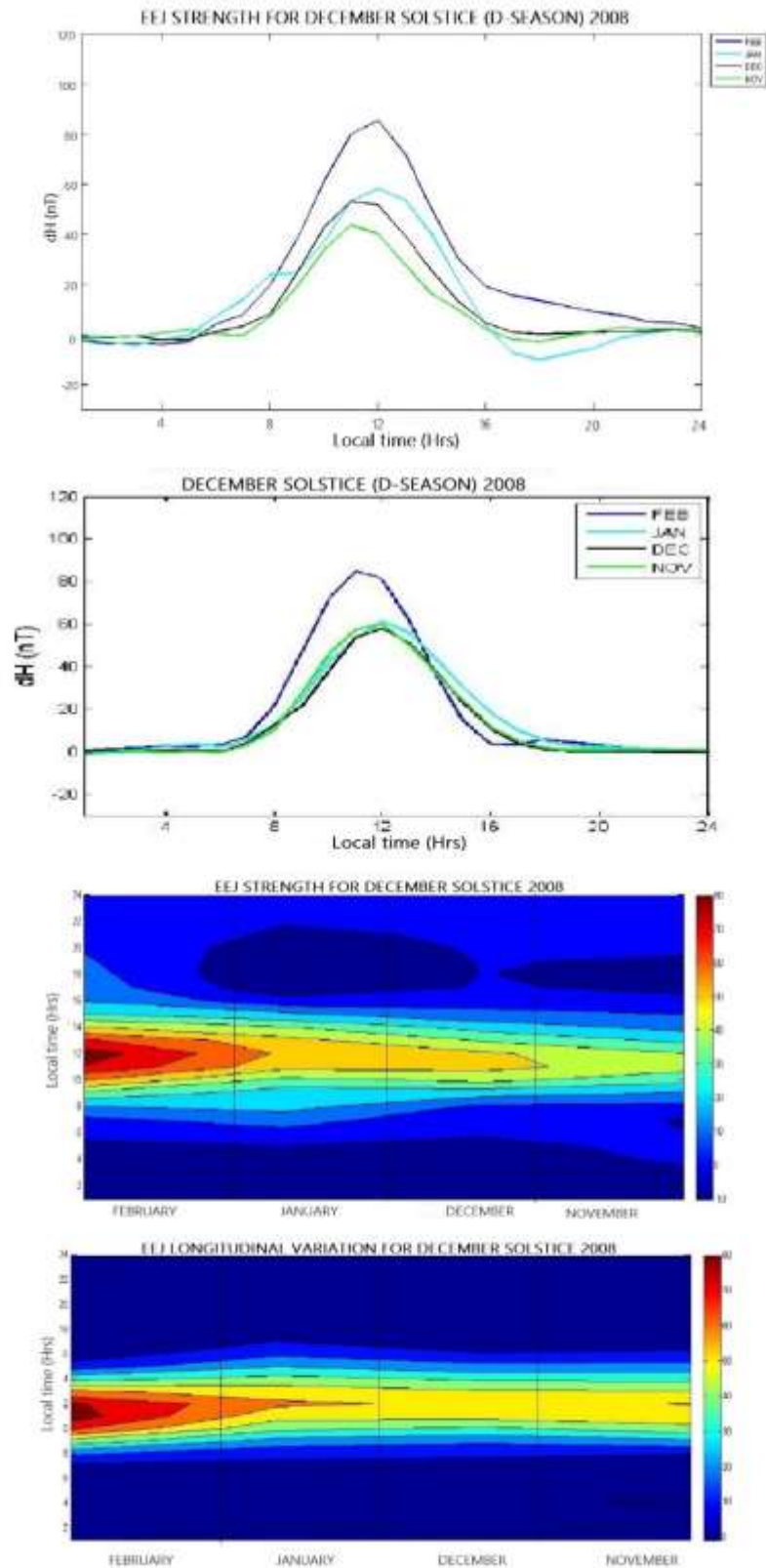


Figure 13: EEJ variation for December solstice (D-Season)

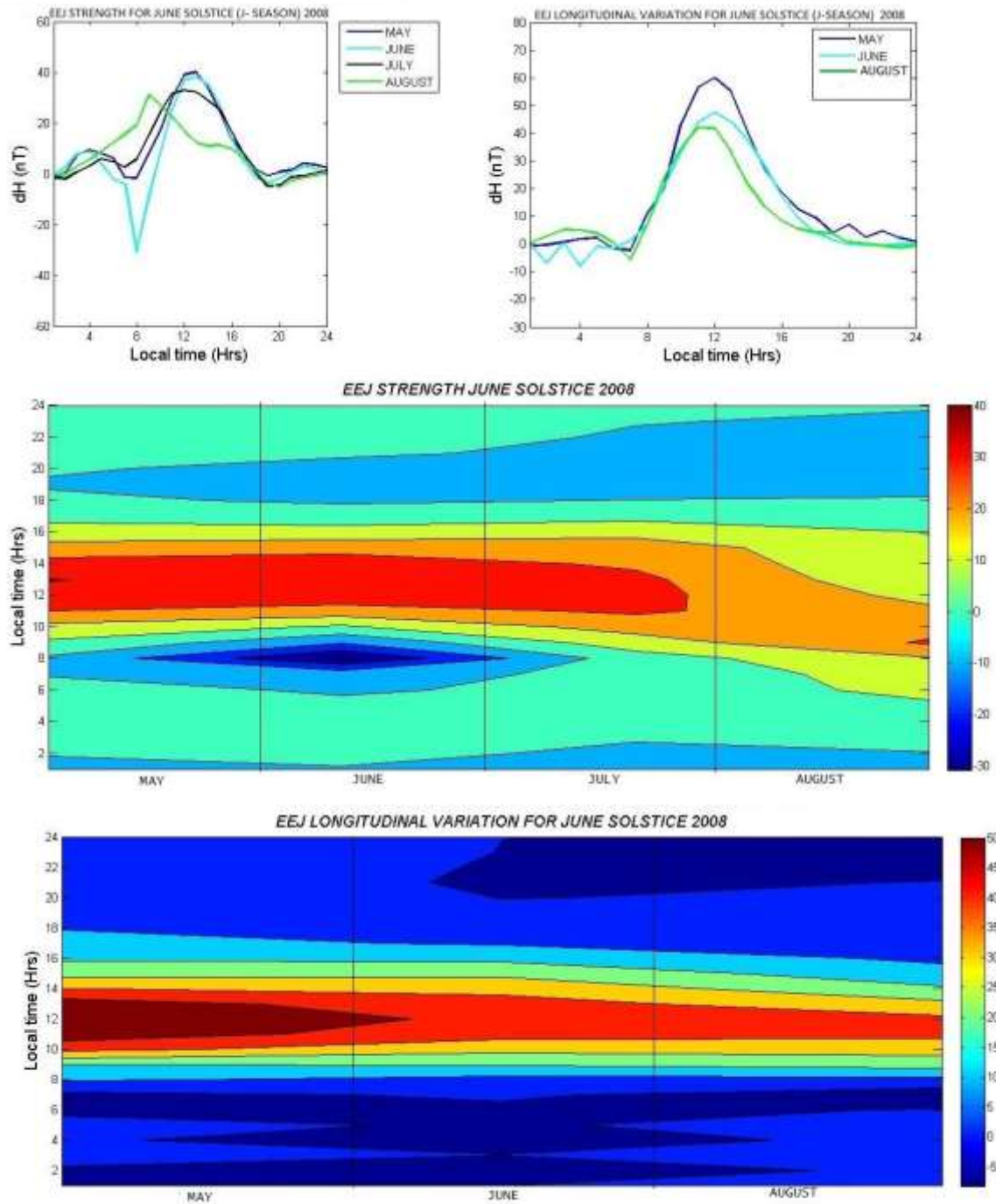


Figure 14: EEJ variation for June Solstice (J-Season)

The result shows a steady increase in dH at pre-sunrise reaching a peak around local noon almost in a regular pattern and decreases at post-sunset. These features are in conformity with the works of Rastogi and Iyer (1976). The $S_q(H)$ variation pattern agrees with the earlier works of Onwumechilli (1960)

and Matshushita (1969) and can be attributed to the variabilities of ionospheric processes and physical structure such as conductivity and wind structure, which are generally responsible for $S_q(H)$ variation. The variation during the daytime which is always higher than nighttime for all the stations is also attributed to the aforementioned ionospheric process and as well as

enhancement dynamo action at their respective regions (Onwumechilli, 1997). *DAV* with a minimum geomagnetic latitude displaying maximum dH for diurnal variation is consistent with the results of Chapman (1951), that latitudinal variation (*EEJ* strength) is expected to be maximum at 0° dip latitude and a continuous decrease both on the southern and northern hemispheres of the magnetic equator until the latitude that defines the edge of the electrojet belt. The *EEJ* strength for all stations within the same longitude is seen to differ, with *DAV* also having the highest value of *EEJ* strength than any other observatory as a result of its high difference in *EEJ* influence on it from stations outside the *EEJ* belt both on the northern (*ASB*) and southern (*CKT*) hemispheres. The *EEJ* strength is a measure of the difference of *EEJ* influence on stations within the *EEJ* belt and those outside either on the northern or southern hemispheres. Thus, latitudinal variation of dH on all stations gives the *EEJ* strength. This study shows that the strength of *EEJ* and its width has been established to change with longitude along the $96^\circ mm$ and $210^\circ mm$ which is consistent with the results obtained by Onwumechilli, 1997. Furthermore, Rastogi (1962) and Jadhav, et al. (2002) studied the *EEJ* strength along the Indian and American sector and showed that it varies with longitude. Rabiou et al. (2011) also revealed that along the African sector, the strength appears weaker at the western sector than in the eastern sector. This west-east asymmetrical behavior in *EEJ* strength in the African sector is further confirmed by Yizengaw et al. (2014) using data from an array of different magnetometers.

The difference in peak time of dH across all stations in the entire months of the year according to Chandra et al. (2000), may be connected with the combined effect of the peak electron density and electric field. The highest dH for longitudinal variation as seen in *DAV* ($108nT$) with its peak at 1200LT can be attributed to the presence of higher electric current (equatorial electrojet) in the ionosphere flowing over *DAV*. Thus, this high magnitude at *DAV* could possibly be due to a greater width of the electrojet over it.

The monthly mean variation follows from the diurnal variation of the *IQDs* in that month. Where the highest dH value is $92nT$ (*DAV* and also *TIR*) occurring during the September equinox and the next value to it is $87nT$ (*YAP* and *CEB*) occurring during the March equinox. These values confirm that the dH during the equinoctial months is higher than solstice months for both longitudinal variation and latitudinal variation.

The seasonal variation of $S_q H$ in general terms has a higher value during equinoctial season than in the solstices. The possible mechanisms responsible for this pattern is the presence of greater solar dynamo processes in the Equinoctial months. Chapman and Raja Rao (1965) and Chandra et al. (1971) also reported greater equinoctial maxima from their observed seasonal variations. Chandra et al. (1971) attributed equinoctial maximum to the more intense $S_q H$ which is narrower at the equinoxes.

Though the mechanisms of seasonal variations in *EEJ* current is still at an expository stage, Tarpley (1973) described the seasonal behavior by establishing that the foci of the solar quiet (S_q) current system in both southern and northern hemisphere

shifts towards the equator during equinox and the poles shift during solstice. He suggested that the actions of the S_q foci are probably due to the variations in the wind driving the ionospheric dynamo. Moreover, seasonal variations may also be caused by other several factors. Some of which according to Fang et al. (2008) are explained on the following basis: Seasonal variation of the solar zenith angle was observed to modulate solar energy fluxes, which in turn controls the ionospheric ionization and thereby affect E region electron density structure. Attenuation of solar ionization radiation at a given altitude below the peak of the E layer where the maximum electrojet current lies however has a strong exponential dependency on the solar zenith angle cosine, making the plasma density below the E region peak principally sensitive to variations in solar zenith angle. The noontime zenith angle is generally bigger during solstices than in equinoxes, with little exceptions. Hence, the seasonal dependence of the solar zenith angle may contribute to the equinoctial maxima in the *EEJ* current strength.

This result shows that the *CEJ* events magnitude and occurrence is greater during the pre-sunset than in pre-sunrise hours of the day in all months. Therefore the *CEJ* events were observed when there are weaker S_q currents. Such similar *CEJ* events at equatorial stations have been extensively reported in the earlier works of Gouin and Mayaud (1967). They attributed *CEJ* phenomenon to the stronger westward current that exceeds the global eastward S_q current this is evident in May 2008.

Immel et al., (2006) conclude that neutral winds in the lower atmosphere influence and modulate the E region dynamo to produce spatial variability approximately 1,000 Km scales. Other causes of *EEJ* variability suggested by earlier works are: i) the variations in tidal strength (Stenin, 1975) and the sharp longitudinal gradients in the diurnal non-migrating tides (DE2 and DW2) between the longitudes over 15° separation (Anderson et al., 2009). ii) the day to day variability of zonal winds Fang et al. (2008). iii) the day to day variability in semidiurnal tide at lower thermosphere, modulated by interactions at planetary wave periodicities (Fuller-Rowell et al., 2008). iv) and the modulation of ionospheric dynamo in the middle atmosphere through the excitation of solar non-migrating tides in the troposphere (Jin et al., 2011).

CONCLUSION

Conclusively, it was observed from the results of this study that the longitudinal and latitudinal geomagnetic field variation during solar quiet condition was obtained for the 11 selected stations within the $96^\circ mm$ and $210^\circ mm$ through which the diurnal transient monthly and seasonal variation of *EEJ* was successfully studied. The strength of *EEJ* at stations within the specified longitude was seen to differ where the minimum *EEJ* strength was observed during the December solstice at *ILR* observatory and maximum *EEJ* strength was observed during September equinox at *DAV* and *YAP* observatory which are also having the highest longitudinal variation of dH . Therefore it was concluded from the results gotten that the *EEJ* value at equinoxes is higher than at solstices which is in conformity and agreement with the work of Akpaneno and Adimula (2015) and is due to the presence of greater solar dynamo processes in the Equinoctial months

REFERENCES

- Akpaneno, A. F. and Adimula, I. A. (2015). Variability of H component of the geomagnetic field at some equatorial electrojet stations. *Sun and Geospher* 10:65-77
- Alex, S., Jadhav, L., and Roa, D.R.K. (1992). Complexity in the Variation of component (D) of the geomagnetic field in the Indian region. *Geol. Soc. Indian Man*; 24:263-274
- Anderson, D., Arango-Pradere, E., and Scherliess, L. (2009). Comparing daytime equatorial $E \times B$ drift velocities and TOPEX/TEC observations associated 4-cell non-migrating tidal structure. *Ann Geophys.* 27: 2861-2867.
- Bartels, J., and Johnston, H.F.. (1940). Geomagnetic tides in horizontal intensity at Huancayo. *Terr. Magn. Atmos. Electr.* **45**, 269–308
- Bhargava, B.N., and Sastri, N.S., (1977). A comparison of days with and without occurrence of counter electrojet afternoon events in the Indian region. *Ann. Geophys.* **33**, 329–333
- Blanc, M., and Richmond, A.D., (1980). The ionospheric disturbance dynamo. *J. Geophys. Res.* **85**(A4), 1669–1686
- Bolaji, O. S., Oyeyemi, E. O., Fagundes, P. R., deAbreu, A. J., deJesus, R., Rabiú, A. B., and Yoshikawa, A. (2014). Counter Electrojet Events using Ilorin Observations during a Low Solar Activity Period, *The African Review of Physics*, 9, 361–376.
- Campbell, W. H. (2003). Introduction to geomagnetic fields (2nd ed.). New York: [Cambridge University Press](#). ISBN 978-0-521-52953-2.
- Chapman, S. (1951). The equatorial electrojet as detected from the abnormal electric current distribution above Huancayo and elsewhere. *Arch. Meteorol. Geophys. Bioclimatol.* **A4**: 368-392.
- Chapman, S., and Raja Rao, K. S. (1965). Some phenomena of the upper Atmosphere *J. Atmos. Terr. Phys.* 27, 559-581
- Chandra, H., Mistra, R. K. and Rastogi, R. G. (1971) *Planet. Space Sci.* 19, 1497-1503.
- Chandra, H., Sinha, H. S. S. and Rastogi, R. G. (2000). Equatorial electrojet studies from rocket and ground measurements. *Earth Planets Space.* 52, 11-120
- Egedal, J. (1947). The magnetic diurnal variation of the horizontal force near the equator; *Terr. Magn. Atmos. Electr.*, 52(4), 449-451, doi: 10.1029/TE052i004p00449
- Fang, T. W., Richmond, A. D., Liu, J. Y. and Maute, A. (2008). Wind dynamo effects on ground magnetic perturbation and vertical drifts. *J. Geophys. Res.* 113: A11313.
- Fang, T. W., Richmond, A. D., Liu, L. Y. and Maute, A., Lin, C. H., Chen, C. H., and Harper, B. (2008). Model simulation of the equatorial electrojet in the Peruvian and Philippine sectors. *J. Atm. Sol. Terr. Phys.* 70, 2203-2211
- Fejer, B.G., Olson, M.E., Chau, J.L., Stolle, C., Lühr, H., Goncharenko, L.P., Yumoto, K., and Nagatsuma, T. (2010). Lunar dependent equatorial ionospheric electrodynamic effects during sudden stratospheric warmings. *J. Geophys. Res.* **115**, A00G03 doi:10.1029/2010JA015273
- Forbes, J.M., and Lindzen, R.S.. (1976b). Atmospheric solar tides and their electrodynamic effects, II the equatorial electrojet. *J. Atmos. Terr. Phys.* **38**, 911–920
- Forbes, J. M., (1981). The equatorial electrojet. *Rev. Geophys.*, 19, 469-504
- Fuller-Rowell, T.J., Millward, G.H, Richmond, A.D., and Codrescu, M.V., (2002). Storm-time changes in the upper atmosphere at low latitudes. *J. Atmos. Sol.-Terr. Phys.* **64**, 1383–1391
- Fuller-Rowell, T.J., Akmaev, R. A., Wu, F., Anghel, A., Maruyama, N., Anderson, D. N., Codrescu, M. V., Iredell, M., Moorthi, S., Juang, H. M., Hou, Y. T., Millard, G. (2008). Impact of terrestrial weather on the upper atmosphere. *Geophys., Res., Lett.* 35: L09808.
- Gouin, P., Mayaud, P. N. (1967). *Ann. Geophys.* 23, 41-47.
- Gurubaran S., (2002). The equatorial counter electrojet: Part of a worldwide current system? *Geophys. Res. Lett.* **29**, 1337 doi:10.1029/2001GL014519
- Hanuis, C., Mazaudier, C., Vila, P., Blanc, M., and Crochet, M.. (1983). Global dynamo simulation of ionospheric currents and their connection with the equatorial electrojet and counter electrojet: a case study. *J. Geophys. Res.* **88**, 253–270
- Hutton, R. (1962). The interpretation of low latitude geomagnetic daily variations. *Ann. Geophys.*, **26**: 927-933.
- Immel, T. W., Sagawa, E., Eglund, S. L., Henderson, S. B., Hagan, M. E., Mende, S. B., Frey, H. U., Sweson, C. M. and Paxton, L. J. (2006). Control of equatorial ionospheric morphology by atmospheric tides. *Geophys. Res. Lett.* 33: L15108
- Jadhav, G., Rajaram, M., and Rajaram, R. (2002). A detailed study of equatorial electrojet phenomenon using oersted satellite observations, *J. Geophys. Res.*, 107, 1175, doi:10.1029/2001JA000183.
- Jin, H., Miyoshi, Y., Fujiwara, H., Shinagawa, H., Terada, K., Terada, N., Ishii, M., Otsuka, Y. and Saito, A. (2011). Vertical connection from the tropospheric activities to the ionospheric longitudinal structure simulated by a new Earth's whole atmosphere-ionosphere coupled model. *J. Geophys. Res.* 116: A01316
- Khshaba, I.A., and Ghamry, E., (2015). Longitudinal Dependence and Seasonal Effect of Equatorial Electrojet using MAGDAS Data. *J. Geol. Geophys* 5:235. Doi: 10.4172/2381-8713.1000235

- Kikuchi, T., Hashimoto, K.K., Kitamura, T.-I., Tachihara, H., and Fejer, B. (2003). Equatorial counter-electrojets during substorms. *J. Geophys. Res.* **108**(A11), 1406 doi:10.1029/2003JA009915
- Kikuchi, T., Hashimoto, K.K., and Nozaki K., (2008). Penetration of magnetospheric electric fields to the equator during a geomagnetic storm. *J. Geophys. Res.* **113**, A06214 doi:10.1029/2007JA012628
- Labitzke, K., and Van Loon H., (1993). Some recent studies of probable connections between solar and atmospheric variability: *Annals of Geophysical Research*
- Le Huy, M., and Amory-Mazaudier, C., (2005). Magnetic signature of the ionospheric disturbance dynamo at equatorial latitudes: *dyn. J. Geophys. Res.* **110**, A10301 doi:10.1029/2004JA010578
- Marriott, R.T., Richmond, A.D., and Venkateswaran, S.V., (1979). The quiet-time equatorial electrojet and counter-electrojet. *J. Atmos. Sol.-Terr. Phys.* **31**, 311–340
- Matsushita, S. (1969). Dynamo currents, winds, and electric fields. *Radio Sci.*, **4**: 771-776.
- Mayaud, P.N. (1977). The equatorial counter-electrojet—a review of its geomagnetic aspects. *J. Atmos. Terr. Phys.* **39**, 1055–1070
- Muralikrishna, P., and Kulkarni, V.H., (2008). Modeling the meteoric dust effect on the equatorial electrojet. *Adv. Space Res.* **42**, 164–170 (2008). doi:10.1016/asr.2007.11.019
- Okeke, F. N. and Onwumechili, C. A., (1995). Preliminary analysis of geomagnetic day to day variations in the equatorial zone. *AIP conference proceedings* 320, 49(1995): doi
- Onwumechili, C. A. (1960). Fluctuations in the geomagnetic field near the magnetic equator. *J. Atmos. Terr. Phys.*, **17**: 286-294.
- Onwumechili, C. A. (1997). *The Equatorial Electrojet*. Gordon and Breach Science Publishers, the Netherlands, 627 pp.
- Oyekola, S. O. (2009). Equatorial F-region vertical ion drifts during quiet solar maximum. *Advances in Space Research*, **43**, 1950-1956.
- Prolss, G. W. (1987). Storm-induced changes in the thermospheric composition at middle latitudes. *Planet. Space Sci.* **35**, 807-811.
- Rabiu, A. B., Folarin, O. O., Uozumi, T., Abdul Hamid, N. S., and Yoshikawa, A., (2017). Longitudinal variation of equatorial electrojet and the occurrence of its counter electrojet. *Ann. Geophys.*, **35**, 535-545, doi:10.5194/angeo-35-535-2017.
- Rabiu, A. B., (2015). Terrestrial and extraterrestrial Divine nexus for man's comfort. *Inaugural lecture series to; FUTA BDC*, 17-19
- Rabiu, A. B., and Nagarajan, N., (2006). A paper on 'The morphology of equatorial electrojet over Indian sector'. Department of Physics, Federal University of Technology, Akure, Nigeria. National Geophysical Research Institute, Hyderabad 500 007, India.
- Rabiu, A. B., Yumoto, K., Falayi, E. O., Bello, O. R., and MAGDAS/CPMN Group (2011). *Ionosphere over Africa: Results from geomagnetic field measurement during international Heliophysical Year IHY*, *Journal of Sun and Geosphere*, **6**, 61–64.
- Raghavarao, R., and Anandarao, B.G. (1980). Vertical winds as a plausible cause for equatorial counter electrojet. *Geophys. Res. Lett.* **7**, 357–360
- Rastogi, R. G. (1962). Longitudinal variation in the equatorial electrojet. *J. Atmos. Terr. Phys.*, **24**, 1031–1040.
- Rastogi, R.G., and Patel, V.L. (1975). Effect of interplanetary magnetic field on ionosphere over the magnetic equator. *Proc. Indian Acad. Sci.* **A82**, 121–141
- Rastogi, R.G. (1977). Geomagnetic storms and electric fields in the equatorial ionosphere. *Nature* **268**, 422–424
- Rastogi, R.G. (1997). Midday reversal of equatorial ionospheric electric field. *Ann. Geophys.* **15**, 1309–1315
- Rastogi, R.G. (1974). Lunar effects in the counter electrojet near the magnetic equator. *J. Atmos. Terr. Phys.* **36**, 167–170
- Rastogi, R.G., Alex, S., and Patil, A., (1994). Seasonal variations of geomagnetic D, H and Z fields at low latitudes. *J. Geomagn. Geoelectr.* **46**, 115–126
- Rastogi, R. G., and Iyer, K. N. (1976). Quiet day variation of geomagnetic H-field at low latitudes. *J. Geomagn. Geoelectr.*, **28**: 461-479.
- Richmond, A. D., (1973). Equatorial electrojet I. Development of a model including winds and instabilities. *J. Atmos. Terr. Phys.*, **35**, 1083-1103
- Roy, M. and Rao, D. R. K., (1998) Frequency dependence of equatorial electrojet effect on geomagnetic micropulsations, *Earth Planets Space*, **50**, 847–851,
- Sastri, N.S., and Arora, B.R. (1981). Lunar modulation of the occurrence frequency of the afternoon counter-electrojet events at Trivandrum. *Planet. Space Sci.* **10**, 1091–1094
- Sridharan, S., Sathishkumar, S., Gurubaran, S. (2009). Variability of mesospheric tides and equatorial electrojet strength during major stratospheric warming events. *Ann. Geophys.* **27**, 4125–4130
- Stenin, R. J. (1975). Problems of identifying lunar geomagnetic effects at Huancayo. *J. Geomagn. Geoelectr.* **27**: 409-424
- Stening, R.J., (1977b). Magnetic variations at other latitudes during reverse equatorial electrojet. *J. Atmos. Terr. Phys.* **39**, 1071–1077
- Stening, R.J., Meek, C.E., and Manson, A.H. (1996). Upper atmosphere wind systems during reverse equatorial electrojet events. *Geophys. Res. Lett.* **23**, 3243–3246

- Takeda, M., and Maeda, H.. (1981). Three-dimensional structure of ionospheric currents, 2: currents caused by semidiurnal tidal winds. *J. Geophys. Res.* **86**, 5861–5867
- Takeda, M., and Maeda, H., (1980b). Equivalent Sq current system at occasions of the equatorial counter electrojet. *J. Geomagn. Geoelectr.* **32**, 297–301
- Tarpley, J. D. (1973). Seasonal movement of S_q current foci and related effects in the equatorial electrojet. *J. Atmos. Terr. Phys.* **35**, 1063-1071.
- Vineeth, C., Mridula, N., Muralikrishna, P., Kumar, K.K., and Pant, T.K., (2016). First observational evidence for the connection between the meteoric activity and occurrence of equatorial counter electrojet. *J. Atmos. Sol.-Terr. Phys.* **147**, 71–75
- Yamazaki, Y., Yumoto, K., McNamara, D., Hirooka, T., Uozumi, T., Kitamura, K., Abe, S., and Ikeda A., (2012a). Ionospheric current system during sudden stratospheric warming events. *J. Geophys. Res.* **117**, A03334 doi:10.1029/2011JA017453
- Yamazaki, Y., Kosch, M.J., and Emmert, J.T., (2015). Evidence for stratospheric sudden warming effects on the upper thermosphere derived from satellite orbital decay data during 1967–2013. *Geophys. Res. Lett.* **42**, 6180–6188 doi:10.1002/2015GL065395
- Yizengaw, E., Moldwin, M. B., Zesta, E., Biouele, C. M., Dantie, B., Mebrahtu, A., Rabiou, B., Valladares, C. F., and Stoneback, R. (2014). The longitudinal variability of equatorial electrojet and vertical drift velocity in the African and American sectors, *Ann. Geophys.*, **32**, 231–238, doi:10.5194/angeo-32-231-2014.
- Yumoto, K. and The CPMN Group, (2001). Characteristics of Pi 2 magnetic pulsations observed at the CPMN stations. A review of the STEP results, *Earth Planet Space*, Vol. 53pp. 981-992
- <http://www.amateur-radio-wiki.net/index.php?title=propagation>
- <http://www.en.wikipedia.org/wiki/ionosphere>
- http://www.navipedia.net/index.php/Nequick_ionospheric_model